

The graph structure of the generalized discrete Arnold Cat map

Chengqing Li, Kai Tan, Bingbing Feng, Jinhu Lü

Abstract—Chaotic dynamics is an important source for generating pseudorandom binary sequences. F. Chen, et al. precisely derived period distribution of the generalized discrete Arnold Cat map in Galois ring \mathbb{Z}_{2^e} using Hensel’s lifting approach (IEEE Trans. Inf. Theory, vol. 59, no. 5, pp. 3249–3255, 2013). However, the paper confused the period of point (state) with that of the whole map and overestimated impact of the work in chaos theory and cryptographic applications. This paper aims to clarify the problem by disclosing its real structure of the generalized discrete Arnold Cat map in any digital domain.

Index Terms—arithmetic domain, chaotic cryptography, generalized Cat map, pseudorandom number sequence, period distribution.

I. INTRODUCTION

PERIOD and cycle distribution of chaotic maps is a fundamental research topic in chaotic dynamics and is also important for their cryptographic applications, e.g. chaotic cryptography [1], [2], hashing scheme [3], PRNS [4], [5], random perturbation [6], surveillance [7]. Arnold’s cat map

$$f(x, y) = (x + y, x + 2y) \pmod{1}$$

is one of the most famous chaotic maps, named after Vladimir Arnold, who heuristically demonstrated its stretching (mixing) effects using an image of a cat in [8, Fig. 1.17]. The original cat map can be attributed as the general matrix form

$$f(\mathbf{x}) = (\Phi \cdot \mathbf{x}) \pmod{N}, \quad (1)$$

where N is a positive integer, \mathbf{x} is a vector of size $n \times 1$, and Φ is a matrix of size $n \times n$. The determinant of the transform matrix Φ in Eq. (1) is one, so the original cat map is area-preserving. Keeping such fundamental characteristic unchanged, Arnold Cat map can be generalized via various strategies: changing the scope (domain) of the elements in Φ [9]; extending transform matrix to 2-D, 3-D and even any higher dimension [10]; modifying the modulo N [11].

Among all kinds of generalizations of Cat map, the one in 2-D integer domain received most intensive attentions due

to its direct application in permuting position of elements of image data, which can be represented as

$$f \begin{bmatrix} x_n \\ y_n \end{bmatrix} = \begin{bmatrix} x_{n+1} \\ y_{n+1} \end{bmatrix} = \mathbf{C} \cdot \begin{bmatrix} x_n \\ y_n \end{bmatrix} \pmod{N}, \quad (2)$$

where

$$\mathbf{C} = \begin{bmatrix} 1 & p \\ q & 1 + p \cdot q \end{bmatrix}, \quad (3)$$

$x_n, y_n \in \mathbb{Z}_N$, and $p, q, N \in \mathbb{Z}^+$. In this paper, we refer to Cat map (2) as the generalized discrete Arnold Cat map (GDCM). In [12], the upper and lower bounds of the period of GDCM (2) with $(p, q) = (1, 1)$ are theoretically derived. In [13], the corresponding properties of GDCM (2) with (p, q, N) satisfying some constrains are further disclosed. In [14]–[17], F. Chen systematically analyzed the precise period distribution of GDCM (2) with any parameters. The whole analyses are divided into three parts according to influences on algebraic properties of $(\mathbb{Z}_N, +, \cdot)$ imposed by N : a Galois field when N is a prime [15]; a Galois ring when N is a power of a prime [14], [16]; a commutative ring when N is a common composite [17]. According to the analysis methods adopted, the second case is further divided into two sub-cases $N = p^e$ and $N = 2^e$, where p is a prime larger than or equal to 3 and e is an integer. From the viewpoint of real applications in digital devices, the case of Galois ring \mathbb{Z}_{2^e} is of most importance since it is isomorphic to the set of numbers represented by e -bit fixed-point arithmetic format with operations defined in the standard for computer arithmetic.

In the abstract part of [16], it was claimed that “Our results have impact on both chaos theory and its applications as they not only provide design strategy in applications where special periods are required, but also help to identify unstable periodic orbits of the original chaotic cat map.” Other references like [13] also hold similar opinions on impact of the knowledge about period distribution of Cat map. The paper analyzes evolution properties of the internal structure of GDCM (2) with incremental increase of e , which can negate the two impacting points in the statement of [16].

The rest of this paper is organized as follows. Section II presents some properties on structure of the generalized discrete Arnold Cat map. In Sec. III, we give the concluding remarks.

This work was supported by the National Natural Science Foundation of China (no. 61772447, 61532020).

C. Li is with College of Computer Science and Electronic Engineering, Hunan University, Changsha 410082, Hunan, China (DrChengqingLi@gmail.com).

K. Tan and B. Feng are with College of Information Engineering, Xiangtan University, Xiangtan 411105, Hunan, China.

J. Lü is with School of Automation Science and Electrical Engineering, Beihang University, Beijing 100083, China

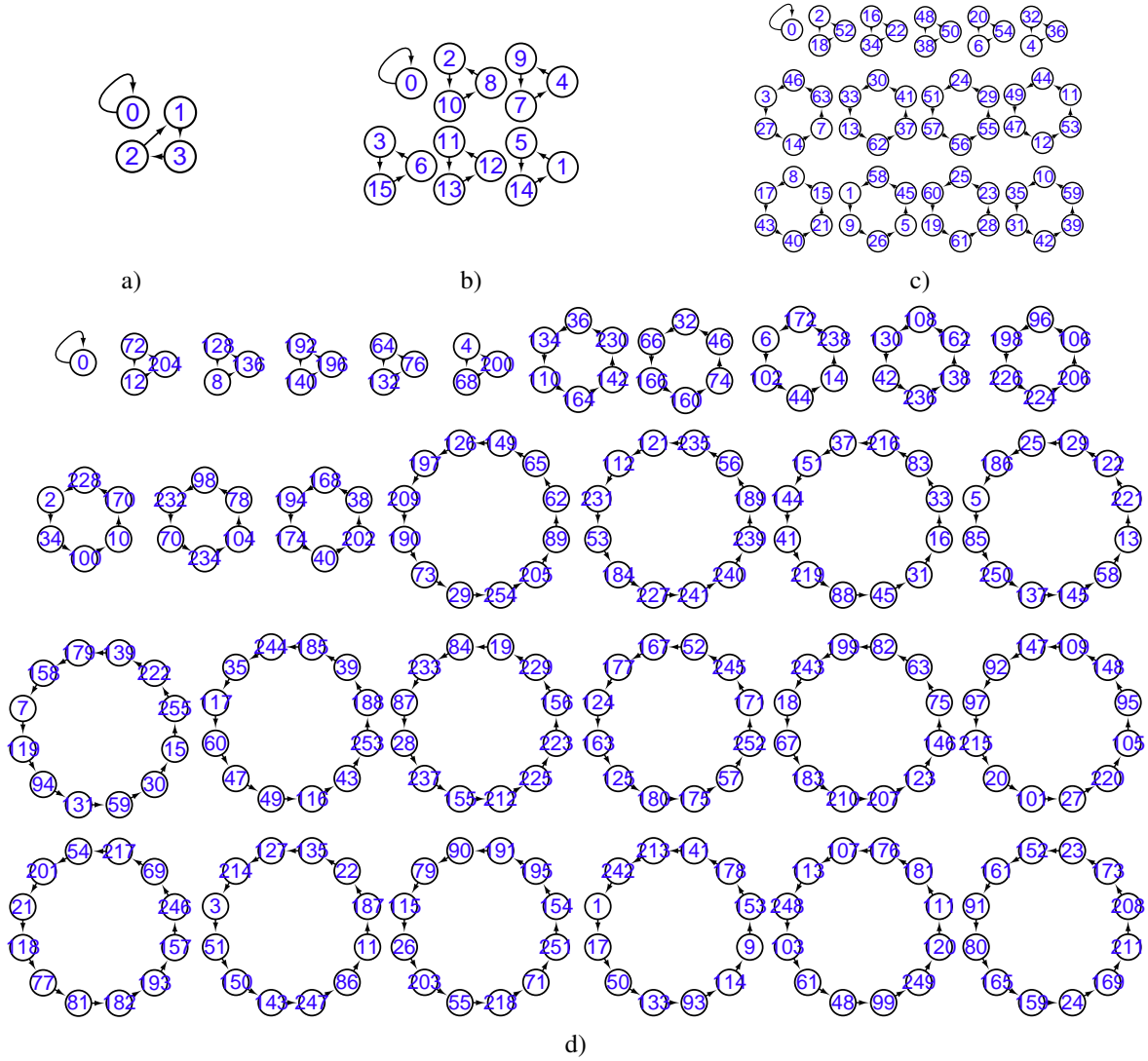


Fig. 1: Functional graphs of generalized Arnold maps in \mathbb{Z}_{2^e} where $(p, q) = (1, 1)$: a) $e = 1$; b) $e = 2$; c) $e = 3$; d) $e = 4$.

II. MAIN RESULTS

Property 1. *The representation form of T is determined by parity of p and q :*

$$T = \begin{cases} 2^k, & \text{if } 2 \mid p \text{ or } 2 \mid q; \\ 3 \cdot 2^{k'}, & \text{if } 2 \nmid p \text{ and } 2 \nmid q. \end{cases} \quad (4)$$

where $k \in \{0, 1, \dots, e\}$, $k' \in \{0, 1, \dots, e-2\}$.

In [16], the representation form of the possible period of GDCM (2) with $N = 2^e$, T , is obtained as shown in Property 1. Furthermore, the relationship between T and the number of different Cat maps possessing the period, N_T , is

precisely derived:

$$N_T = \begin{cases} 1 & \text{if } T = 1; \\ 3 & \text{if } T = 2; \\ 2^{e+1} + 12 & \text{if } T = 4; \\ 2^{e-1} + 2^e & \text{if } T = 6; \\ 2^{e+k-2} + 3 \cdot 2^{2k-2} & \text{if } T = 2^k, k \in \{3, 4, \dots, e-1\}; \\ 2^{2e-2} & \text{if } T = 2^e; \\ 2^{e+k-1} & \text{if } T = 3 \cdot 2^k, k \in \{0, 2, 3, \dots, e-2\}, \end{cases} \quad (5)$$

where $e \geq 4$.

When $e = 3$,

$$N_T = \begin{cases} 1 & \text{if } T = 1; \\ 3 & \text{if } T = 2; \\ 2^{e-1} & \text{if } T = 3; \\ 2^{e+1} + 12 & \text{if } T = 4; \\ 2^{e-1} + 2^e & \text{if } T = 6; \\ 2^{2e-2} & \text{if } T = 8, \end{cases}$$

which cannot be presented as the general form (5) as [16, Table III], e.g. $2^{2e-2} \neq 2^{e+k-2} + 3 \cdot 2^{2k-2}$ when $e = k = 3$. From Eq. (5), one can see that there are $(1+3+2^{e-1}+2^{e+1}+12+2^{e-1}+2^e) = 2^{e+2}+16$ generalized Arnold maps whose periods are not larger than 6, which is a huge number for ordinary digital computer, where $e \geq 32$. Generating function of the sequence can be represented as

$$X(t) = \frac{g_x(t)}{f(t)} \quad (6)$$

and

$$Y(t) = \frac{g_y(t)}{f(t)}, \quad (7)$$

where

$$\begin{bmatrix} g_x(t) \\ g_y(t) \end{bmatrix} = \begin{bmatrix} -1-pq & p \\ q & -1 \end{bmatrix} \cdot \begin{bmatrix} x_0 \\ y_0 \end{bmatrix} \cdot t + \begin{bmatrix} x_0 \\ y_0 \end{bmatrix}, \quad (8)$$

and

$$f(t) = t^2 - ((pq+2) \bmod 2^e) \cdot t + 1. \quad (9)$$

Functional graph of GDCM (2) can provide direct perspective on its structure. The associate *functional graph* F_e can be built as follows: the N^2 possible states are viewed as N^2 nodes; the node corresponding to $\mathbf{x}_1 = (x_1, y_1)$ is directly linked to the other one corresponding to $\mathbf{x}_2 = (x_2, y_2)$ if and only if $\mathbf{x}_2 = f(\mathbf{x}_1)$. To facilitate visualization as a 1-D network data, every 2-D vector in GDCM (2) is transformed by a bijective function $z_n = x_n + (y_n \cdot N)$. To describe how the functional graph of GDCM (2) change with the arithmetic precision e , let

$$z_{n,e} = x_{n,e} + (y_{n,e} \cdot 2^e), \quad (10)$$

where $x_{n,e}$ and $y_{n,e}$ denote x_n and y_n of GDCM (2) with $N = 2^e$, respectively.

As a typical example, we depicted the functional graphs of GDCM (2) with $(p, q) = (1, 3)$ in four domains $\{\mathbb{Z}_{2^e}\}_{e=1}^4$ in Fig. 1, where the number inside each circle (node) is $z_{n,e}$ in F_e . From Fig. 1, one can observe some general properties of functional graphs of GDCM (2). Among them, the properties on permutation are concluded in Properties 2, 3.

Property 2. *GDCM (2) defines a bijective mapping on the set $(0, 1, 2, \dots, N^2 - 1)$.*

Proof. As Cat map (2) is area-preserving on its domain, it defines a bijective mapping on \mathbb{Z}_N^2 , which is further transformed into a bijective mapping on \mathbb{Z}_{N^2} by conversion function (10). \square

Property 3. *As for a given N , any node of functional graph of GDCM (2) belongs one and only one cycle, a set of nodes such that GDCM (2) iteratively map them one to the other in turn.*

Proof. Referring to [18, Theorem 5.1.1], the set $(0, 1, 2, \dots, N^2 - 1)$ is divided into some disjoint subsets such that GDCM (2) is a cycle on each subset. \square

As the period of a generalized Cat map on a domain is the least common multiple of the periods of its cycles, the functional graph of a generalized Arnold map possessing a

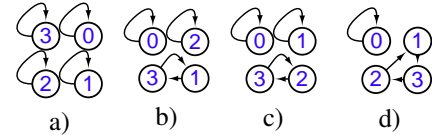


Fig. 2: Four possible functional graphs of GDCM (2) with $N = 2$: a) p and q are both even; b) p is even, and q is odd; c) p is odd, q is even; d) p and q are both odd.

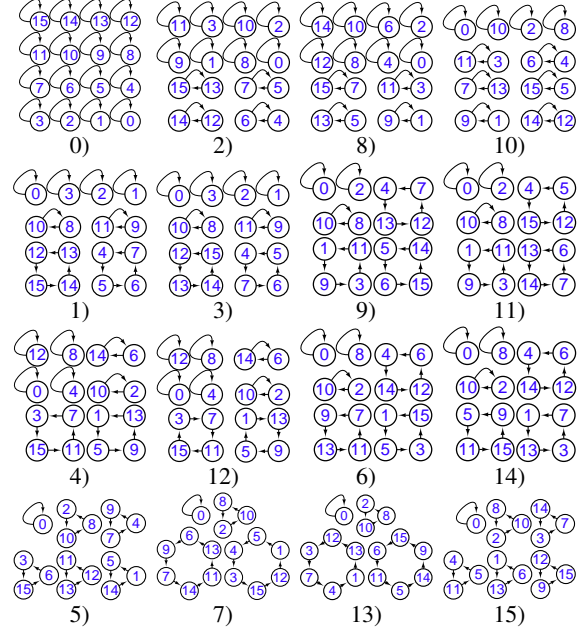


Fig. 3: All possible functional graphs of GDCM (2) with $N = 2^2$, where the subfigure with caption “ i ” is corresponding to (p, q) satisfying $i = p \bmod 4 + (q \bmod 4) \cdot 4$.

large period may be composed of a great number of cycles of very small periods. The whole graph shown in Fig. 1d) is composed of 16 cycles of period 12, 10 cycles of period 6, 1 cycle of period 3, and 1 self-connected cycle. What’s worse, the concrete relationship between the two control parameters of generalized Arnold map and its period is still unknown. Although [16] claimed that “From the design point of view, our results lead to the choice of proper cat maps when a specific period, no matter large or small, is required” as no any positive information can be obtained from Eq. (5) as for proper choice of cat maps owning a specific aperiodicity. As shown in [19], attack on the cryptographic system based on Cat map has no relationship with the amount of the period of the underlying chaotic map.

We found that there exists strong evolution relationship between F_e and F_{e+1} . A node $z_{n,e} = x_{n,e} + y_{n,e}2^e$ in F_e is evolved to

$$\begin{aligned} z_{n,e+1} &= (x_{n,e} + a_n 2^e) + (y_{n,e} + b_n 2^e) 2^{e+1} \\ &= z_{n,e} + (a_n 2^e + y_{n,e} 2^e + b_n 2^{2e+1}), \end{aligned} \quad (11)$$

where $a_n, b_n \in \{0, 1\}$. The relationship between iterated node of $z_{n,e}$ in F_e and the corresponding evolved one in F_{e+1} is described in Property 4. Furthermore, the associated cycle is expanded to up to four cycles as presented in Property 5. Assign (a_{n_0}, b_{n_0}) with one element in set (17), one can obtain

TABLE I: The conditions of (p, q) and the number of their possible cases, N'_T , corresponding to a given T .

T	p	q	N'_T
1	0	0	1
2	$p \bmod 2^e = 2^{e-1}$	$q \bmod 2^{e-1} = 0$	2
	$q \bmod 2^e = 0$	$p \bmod 2^e = 2^{e-1}$	1
3	$p \equiv 1 \pmod 2$	$q \equiv p^{-1}(2^e - 3) \pmod{2^e}$	2^{e-1}
4	$p \equiv 1 \pmod 2$	$q \equiv p^{-1}(2^e - 2) \pmod{2^e}$	2^{e-1}
	$p \equiv 0 \pmod 2, p \not\equiv 0 \pmod 4$	$q \equiv (p/2)^{-1}(2^{e-1} - 1) \pmod{2^{e-1}}$	2^{e-1}
	$p \equiv 1 \pmod 2$	$q \equiv p^{-1}(2^{e-1} - 2) \pmod{2^e}$	2^{e-1}
	$p \equiv 0 \pmod 2$	$q \equiv (p/2)^{-1}(2^{e-1} - 2) \pmod{2^e}$	2^{e-1}
	$p \bmod 2^{e-1} = 2^{e-2}$	$q \bmod 2^{e-2} = 0$	8
6	$p \equiv 1 \pmod 2$	$q \bmod 2^{e-1} = 2^{e-2}$	4
		$q \equiv p^{-1}(2^{e-1} - 3) \pmod{2^e}$	2^{e-1}
		$q \equiv p^{-1}(2^{e-1} - 1) \pmod{2^e}$	2^{e-1}
		$q \equiv p^{-1}(2^e - 1) \pmod{2^e}$	2^{e-1}
$2^k,$ $k \in \{3, 4, \dots, e-1\}$	$p \equiv 1 \pmod 2$	$q \equiv p^{-1}(2^{e-k+1}l - 2) \pmod{2^e}, l \equiv 1 \pmod 2, l \in [1, 2^{k-1} - 1]$	2^{e+k-3}
	$p \equiv 0 \pmod 2$	$q \equiv (p/2)^{-1}(2^{e-k+1}l - 2) \pmod{2^e}, l \equiv 1 \pmod 2, l \in [1, 2^{k-1} - 1]$	2^{e+k-3}
	$p \bmod 2^{e-k+1} = 2^{e-k}$	$q \bmod 2^{e-k} = 0$	2^{2k-1}
	$p \bmod 2^{e-k+1} = 0$	$q \bmod 2^{e-k+1} = 2^{e-k}$	2^{2k-2}
2^e	$p \equiv 1 \pmod 2$	$q \equiv 0 \pmod 4$	2^{2e-3}
	$p \equiv 0 \pmod 4$	$q \equiv 1 \pmod 2$	2^{2e-3}
$3 \cdot 2^k,$ $k \in \{2, 3, \dots, e-2\}$	$p \equiv 1 \pmod 2$	$q \equiv p^{-1}(2^{e-k}l - 3) \pmod{2^e}, l \equiv 1 \pmod 2, l \in [1, 2^k]$	2^{e+k-2}
		$q \equiv p^{-1}(2^{e-k+1}l - 1) \pmod{2^e}, l \equiv 1 \pmod 2, l \in [1, 2^{k-1} - 1]$	2^{e+k-2}

the corresponding cycle in F_{e+1} with the steps given in Property 5. Then, the other element in set (17) can be assigned to (a_{n_0}, b_{n_0}) if it does not ever exist in the set in Eq. (16) corresponding to every assigned value of (a_{n_0}, b_{n_0}) . Every cycle corresponding to different (a_{n_0}, b_{n_0}) can be generated in the same way.

Property 4. If the differences between inputs of GDCM (2) with $N = 2^e$ and that of GDCM (2) with $N = 2^{e+1}$ satisfy

$$\begin{bmatrix} x_{n,e+1} - x_{n,e} \\ y_{n,e+1} - y_{n,e} \end{bmatrix} = \begin{bmatrix} a_n \\ b_n \end{bmatrix} \cdot 2^e, \quad (12)$$

one has

$$\begin{bmatrix} a_{n+1} \\ b_{n+1} \end{bmatrix} = \begin{bmatrix} 1 & p \\ q & 1 + p \cdot q \end{bmatrix} \cdot \begin{bmatrix} a_n \\ b_n \end{bmatrix} + \begin{bmatrix} k_x \\ k_y \end{bmatrix} \pmod 2, \quad (13)$$

$a_n, b_n \in \{0, 1\}$, $k_x = \lfloor k'_x/2^e \rfloor$, $k_y = \lfloor k'_y/2^e \rfloor$, and

$$\begin{bmatrix} k'_x \\ k'_y \end{bmatrix} = \begin{bmatrix} 1 & p \\ q & 1 + p \cdot q \end{bmatrix} \cdot \begin{bmatrix} x_{n,e} \\ y_{n,e} \end{bmatrix}. \quad (14)$$

Proof. According to the linearity of GDCM (2), one can get

$$\begin{aligned} & \begin{bmatrix} x_{n+1,e+1} - x_{n+1,e} \\ y_{n+1,e+1} - x_{n+1,e} \end{bmatrix} \\ &= \begin{bmatrix} 1 & p \\ q & 1 + p \cdot q \end{bmatrix} \begin{bmatrix} x_{n,e+1} - x_{n,e} \\ y_{n,e+1} - y_{n,e} \end{bmatrix} + 2^e \begin{bmatrix} k_x \\ k_y \end{bmatrix} \pmod{2^{e+1}}. \end{aligned} \quad (15)$$

As $k \cdot a \equiv k \cdot a' \pmod m$ if and only if $a \equiv a' \pmod{\frac{m}{\gcd(m,k)}}$ and $a_{n+1,e}, b_{n+1,e} \in \{0, 1\}$, the property can be proved by putting condition (12) into equation (15) and dividing its both sides and the modulo by 2^e . \square

Property 5. Given a cycle $\mathbf{Z}_e = \{z_{n,e}\}_{n=0}^{T_c-1} = \{(x_{n,e}, y_{n,e})\}_{n=0}^{T_c-1}$ in F_e and its any point $z_{n_0,e}$, one has that the cycle to which $z_{n_0,e+1}$ belongs in F_{e+1} is

$$\mathbf{Z}_{e+1} = \{z_{n,e+1}\}_{n=n_0}^{n_0+kT_c-1},$$

where

$$k = \#\{(a_{n_0}, b_{n_0}), (a_{n_0+T_c}, b_{n_0+T_c}), (a_{n_0+2T_c}, b_{n_0+2T_c}), (a_{n_0+3T_c}, b_{n_0+3T_c})\}, \quad (16)$$

$z_{n,e} = z_{n',e}$ for $n \geq T_c$, $n' = n \bmod T_c$, $\{(a_n, b_n)\}_{n=n_0}^{n_0+3T_c}$ are generated by iterating Eq. (13) for $n = n_0 \sim n_0 + 3T_c$, and $\#(\cdot)$ returns the cardinality of a set.

Proof. Given a node in a cycle, (k_x, k_y) in Eq. (13) is fixed, so Eq. (13) defines a bijective mapping on set

$$\{(0, 0), (0, 1), (1, 0), (1, 1)\} \quad (17)$$

as shown in Fig. 4. So, $z_{n,e+1}$ may fall in set $\{z_{j,e+1}\}_{j=n_0}^n$ when and only when $(n - n_0) \bmod T_c = 0$ and $n > n_0$, i.e. the given cycle is went through one more times. \square

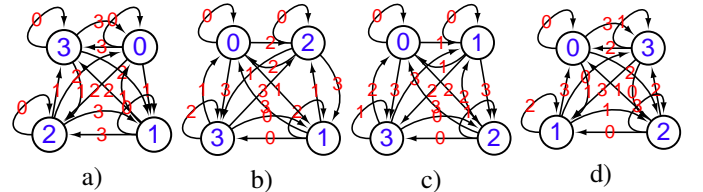


Fig. 4: Mapping relationship between $(a_n + 2b_n)$ and $(a_{n+1} + 2b_{n+1})$ in Eq. (13) with $(k_x + 2k_y)$ shown beside the arrow: a) p and q are both even; b) p is even, and q is odd; c) p is odd, q is even; d) p and q are both odd.

Depending on the number of candidates for (a_{n_0}, b_{n_0}) and the corresponding cardinality in Eq. (16), a cycle of length T_c

TABLE II: The threshold values e_s, T_s under various values of (p, q) .

$e, T_c \backslash q$	1	2	3	4	5	6	7	8	9	10	11	12	13	14	15	16
$p \backslash$																
1	3,6	4,8	4,12	2,4	4,6	5,8	5,12	1,2	3,6	4,8	4,12	2,4	5,6	6,8	6,12	1,2
2	4,8	3,4	5,8	2,2	4,8	3,4	6,8	2,2	4,8	3,4	5,8	2,2	4,8	3,4	7,8	2,2
3	4,12	5,8	3,6	2,4	6,12	4,8	4,6	1,2	4,12	7,8	3,6	2,4	5,12	4,8	5,6	1,2
4	2,4	2,2	2,4	3,2	2,4	2,2	2,4	3,2	2,4	2,2	2,4	3,2	2,4	2,2	2,4	3,2
5	4,6	4,8	6,12	2,4	3,6	7,8	4,12	1,2	5,6	4,8	5,12	2,4	3,6	5,8	4,12	1,2
6	5,8	3,4	4,8	2,2	7,8	3,4	4,8	2,2	5,8	3,4	4,8	2,2	6,8	3,4	4,8	2,2
7	5,12	6,8	4,6	2,4	4,12	4,8	3,6	1,2	8,12	5,8	5,6	2,4	4,12	4,8	3,6	1,2
8	1,2	2,2	1,2	3,2	1,2	2,2	1,2	4,2	1,2	2,2	1,2	3,2	1,2	2,2	1,2	4,2
9	3,6	4,8	4,12	2,4	5,6	5,8	8,12	1,2	3,6	4,8	4,12	2,4	4,6	9,8	5,12	1,2
10	4,8	3,4	7,8	2,2	4,8	3,4	5,8	2,2	4,8	3,4	6,8	2,2	4,8	3,4	5,8	2,2
11	4,12	5,8	3,6	2,4	5,12	4,8	5,6	1,2	4,12	6,8	3,6	2,4	6,12	4,8	4,6	1,2
12	2,4	2,2	2,4	3,2	2,4	2,2	2,4	3,2	2,4	2,2	2,4	3,2	2,4	2,2	2,4	3,2
13	5,6	4,8	5,12	2,4	3,6	6,8	4,12	1,2	4,6	4,8	6,12	2,4	3,6	5,8	4,12	1,2
14	6,8	3,4	4,8	2,2	5,8	3,4	4,8	2,2	9,8	3,4	4,8	2,2	5,8	3,4	4,8	2,2
15	6,12	7,8	5,6	2,4	4,12	4,8	3,6	1,2	5,12	5,8	4,6	2,4	4,12	4,8	3,6	1,2
16	1,2	2,2	1,2	3,2	1,2	2,2	1,2	4,2	1,2	2,2	1,2	3,2	1,2	2,2	1,2	5,2

in F_e is expanded to five possible cases in F_{e+1} : 1) four cycles of length T_c ; 2) one cycle of length $2T_c$ and two cycles of length T_c ; 3) two cycles of length $2T_c$; 4) one cycles of length $3T_c$ and one cycle of length T_c ; 5) one cycle of length $4T_c$. For example, the self-connected cycle in Fig. 1a), “ $0 \rightarrow 0$ ”, is evolved to two cycles in Fig. 1b), “ $0 \rightarrow 0$ ” and “ $(0 + 2^1) = 2 \rightarrow (0 + 2^3) = 8 \rightarrow (0 + 2^1 + 2^3) = 10 \rightarrow 2$ ”. Similarly, another cycle in Fig. 1a), “ $1 \rightarrow 3 \rightarrow 2 \rightarrow 1$ ” is evolved to the other two cycles in Fig. 1b), “ $1 \rightarrow (3 + 2^1 + 2^3) = 13 \rightarrow (2 + 2^3 + 2) = 12 \rightarrow (1 + 2^1) = 3 \rightarrow (3 + 2^1 + 2) = 7 \rightarrow (2 + 2^1) = 4 \rightarrow 1$ ”; “ $(1 + 2^3) = 9 \rightarrow (3 + 2^1 + 2^3 + 2) = 15 \rightarrow (2 + 2^1 + 2) = 6 \rightarrow (1 + 2^1 + 2^3) = 11 \rightarrow (3 + 2^1) = 5 \rightarrow (2 + 2^1 + 2^3 + 2) = 14 \rightarrow 9$ ”. Note that cycle “ $1 \rightarrow 1$ ” in Fig. 2c) is expanded to “ $1 \rightarrow 9 \rightarrow 3 \rightarrow 11 \rightarrow 1$ ” in the subfigure with caption “9)” in Fig. 3, and cycle “ $0 \rightarrow 0$ ” in Fig. 2c) is expanded to three cycles in the same SMN: “ $0 \rightarrow 0$ ”; “ $2 \rightarrow 2$ ”; “ $8 \rightarrow 10 \rightarrow 8$ ”. In addition, the cycle “ $1 \rightarrow 13 \rightarrow 12 \rightarrow 3 \rightarrow 7 \rightarrow 4 \rightarrow 1$ ” in Fig. 1b) is expanded to four cycles of the same length shown in the lower left side of Fig. 1c). So, all the fives possible cases can be found in Fig. 1, 2, 3.

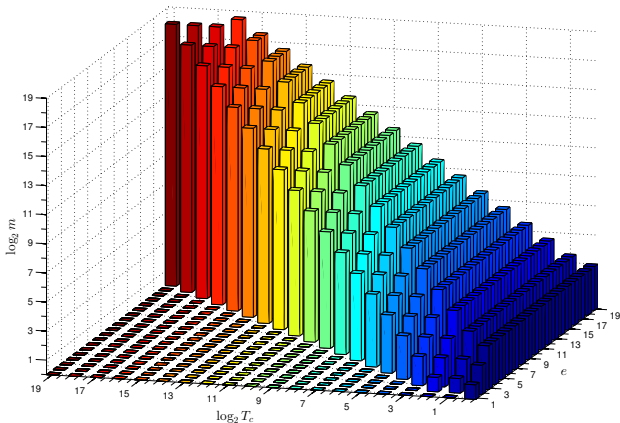


Fig. 5: The cycle distribution of GDCM (2) with $(p, q) = (7, 8)$ in \mathbb{Z}_{2^e} , $e = 1 \sim 19$.

As shown in Property 5, any cycle of F_{e+1} is incrementally expanded from a cycle of F_1 . So, the number of cycles of a given length in F_{e+1} has some relationship with that of the corresponding length in F_e , which is determined by the control parameters p, q . We concluded the relationship as Conjecture 1 and verified it via a large number of random experiments on (p, q) . Table II lists the threshold values e_s, T_s for $p, q \in \mathbb{Z}_{17}$. From Table II, we can see that the two threshold values are both very small compared with the counterparts obtained with the implementation precision of an ordinary computer. Precisely, the value of e_s is less than or equal to $\log_2(16) = 4$ for the cases of ratio $\frac{25}{32}$ in Table II. The period distribution of cycles in F_e follows a power-law distribution of fixed exponent one when e is sufficiently large. The number of cycles of any length is monotonously increased to a constant with respect to e , which is shown in Fig. 5. From Proposition 1, one can see that the number of cycles of various lengths in F_e can be easily deduced from that of F_{e_s} when $e > e_s$, which is demonstrated in Table III.

TABLE III: The number of cycles of period T_c in F_e with $(p, q) = (9, 14)$.

$N_{T_c, e} \backslash T_c$	2^0	2^1	2^2	2^3	2^4	2^5	2^6	2^7
$e \backslash$								
1	2	1	0	0	0	0	0	0
2	2	1	3	0	0	0	0	0
3	2	1	15	0	0	0	0	0
4	2	1	63	0	0	0	0	0
5	2	1	255	0	0	0	0	0
6	2	1	1023	0	0	0	0	0
7	2	1	4095	0	0	0	0	0
8	2	1	16383	0	0	0	0	0
9	2	1	16383	24576	0	0	0	0
10	2	1	16383	24576	49152	0	0	0
11	2	1	16383	24576	49152	98304	0	0
12	2	1	16383	24576	49152	98304	196608	0
13	2	1	16383	24576	49152	98304	196608	393216

In [16], it is assumed that $e \geq 3$ “because the cases when $e = 1$ and $e = 2$ are trivial”. On the contrary, the structure of

functional graph of GDCM (2) with $e = 1$, shown in Fig. 2, plays a fundamental role for that with $e \geq 3$, e.g. the cycles of length triple of 3 in F_e (if there exist) are generated by the cycle of length 3 in F_1 .

Proposition 1. *The n -th iteration of Cat map matrix (3) satisfies*

$$\mathbf{C}^n = \begin{bmatrix} \frac{1}{2}G_n - \frac{A-2}{2}H_n & p \cdot H_n \\ q \cdot H_n & \frac{1}{2}G_n + \frac{A-2}{2}H_n \end{bmatrix}, \quad (18)$$

where

$$\begin{cases} G_n = \left(\frac{A+B}{2}\right)^n + \left(\frac{A-B}{2}\right)^n, \\ H_n = \frac{1}{B} \left(\left(\frac{A+B}{2}\right)^n - \left(\frac{A-B}{2}\right)^n \right), \end{cases} \quad (19)$$

$$B = \sqrt{A^2 - 4} \text{ and } A = p \cdot q + 2.$$

Proof. First, one can calculate the characteristic polynomial of Cat map matrix (3) as

$$\begin{aligned} |\mathbf{C} - \lambda \mathbf{I}| &= \det \begin{bmatrix} 1 - \lambda & p \\ q & p \cdot q + 1 - \lambda \end{bmatrix} \\ &= \lambda^2 - (p \cdot q + 2)\lambda + 1 \\ &= 0. \end{aligned}$$

Solving the above equation, one can obtain two characteristic roots of Cat map matrix:

$$\begin{cases} \lambda_1 = \frac{A+B}{2}, \\ \lambda_2 = \frac{A-B}{2}. \end{cases}$$

Setting λ in $(\mathbf{C} - \lambda \mathbf{I}) \cdot \mathbf{X} = 0$ as λ_1 and λ_2 separately, the corresponding eigenvector $\xi_{\lambda_1} = [1, \frac{A-2+B}{2p}]^\top$ and $\xi_{\lambda_2} = [1, \frac{A-2-B}{2p}]^\top$ can be obtained, which means

$$\mathbf{C} \cdot \mathbf{P} = \mathbf{P} \cdot \Lambda, \quad (20)$$

where $\mathbf{P} = (\xi_{\lambda_1}, \xi_{\lambda_2})$ and

$$\Lambda = \begin{bmatrix} \lambda_1 & 0 \\ 0 & \lambda_2 \end{bmatrix}.$$

From Eq. (20), one has

$$\mathbf{C} = \mathbf{P} \cdot \Lambda \cdot \mathbf{P}^{-1}, \quad (21)$$

where

$$\mathbf{P}^{-1} = \begin{bmatrix} -\frac{A-2-B}{2B} & \frac{p}{B} \\ \frac{A-2+B}{2B} & -\frac{p}{B} \end{bmatrix}.$$

Finally, one can get

$$\begin{aligned} \mathbf{C}^n &= (\mathbf{P} \cdot \Lambda \cdot \mathbf{P}^{-1})^n \\ &= \mathbf{P} \cdot \Lambda^n \cdot \mathbf{P}^{-1} \\ &= \begin{bmatrix} \frac{1}{2}G_n - \frac{A-2}{2}H_n & pH_n \\ qH_n & \frac{1}{2}G_n + \frac{A-2}{2}H_n \end{bmatrix}, \end{aligned}$$

where G_n and H_n are defined as Eq. (19).

Proposition 2. *The period of Cat map (2) over $(\mathbb{Z}_N, +, \cdot)$ is the minimum positive integer n satisfying*

$$\begin{cases} \frac{1}{2}G_n = 1 \pmod{N}, \\ H_n = 0 \pmod{N}. \end{cases}$$

Proof. The proposition can be proved by setting the right hand side of Eq. (18) as the identity matrix of size 2×2 . \square

Lemma 1. *For any positive integer m , the parity of $G_{2^m \cdot s}$ is the same as that of G_s , where s is a given positive integer.*

Proof. Referring to Eq. (19), one has

$$\begin{aligned} G_{2^m \cdot s} &= \left(\frac{A+B}{2}\right)^{2^m \cdot s} + \left(\frac{A-B}{2}\right)^{2^m \cdot s} \\ &= \left(\left(\frac{A+B}{2}\right)^{2^{m-1} \cdot s} + \left(\frac{A-B}{2}\right)^{2^{m-1} \cdot s} \right)^2 \\ &\quad - 2 \left(\frac{A^2 - B^2}{4}\right)^{2^{m-1} \cdot s} \\ &= (G_{2^{m-1} \cdot s})^2 - 2. \end{aligned} \quad (22)$$

When $m = 1$, $G_{2s} = (G_s)^2 - 2$. So the parity of G_{2s} is the same as that of G_s no matter G_s is even or odd. Proceed by induction on m and assume that the lemma hold for any m less than a positive integer $k > 1$. When $m = k$, $G_{2^k \cdot s} = (G_{2^{k-1} \cdot s})^2 - 2$, which means that the parity of $G_{2^k \cdot s}$ is the same as that of $G_{2^{k-1} \cdot s}$ no matter $G_{2^{k-1} \cdot s}$ is even or odd. \square

Lemma 2. *Sequence $\{H_n\}_{n=1}^\infty$ satisfies*

$$H_{2^m \cdot s} = H_s \cdot \prod_{j=0}^{m-1} G_{2^j \cdot s}, \quad (23)$$

where m and s are positive integers.

Proof. This Lemma is proved via mathematical induction on m . When $m = 1$,

$$\begin{aligned} H_{2s} &= \frac{1}{B} \left(\left(\frac{A+B}{2}\right)^{2s} - \left(\frac{A-B}{2}\right)^{2s} \right) \\ &= H_s \cdot G_s. \end{aligned}$$

Now, assume the lemma is true for any m in Eq. (23) less than k . When $m = k$,

$$\begin{aligned} H_{2^k \cdot s} &= \frac{1}{B} \left(\left(\frac{A+B}{2}\right)^{2^k \cdot s} - \left(\frac{A-B}{2}\right)^{2^k \cdot s} \right) \\ &= \frac{1}{B} \left(\left(\frac{A+B}{2}\right)^{2^{k-1} \cdot s} - \left(\frac{A-B}{2}\right)^{2^{k-1} \cdot s} \right) \\ &\quad \cdot \left(\left(\frac{A+B}{2}\right)^{2^{k-1} \cdot s} + \left(\frac{A-B}{2}\right)^{2^{k-1} \cdot s} \right) \\ &= H_{2^{k-1} \cdot s} \cdot G_{2^{k-1} \cdot s}. \end{aligned}$$

\square The above induction completes the proof of the lemma. \square

Lemma 3. If m and s satisfy

$$\begin{cases} \frac{1}{2}G_{2^m \cdot s} = 1 \pmod{2^e}, \\ \frac{1}{2}G_{2^m \cdot s} \neq 1 \pmod{2^{e+1}}, \end{cases} \quad (24)$$

$$(25)$$

one has

$$\frac{1}{2}G_{2^{m+1} \cdot s} = 1 \pmod{2^{e+2}}. \quad (26)$$

Proof. From Eq. (24), one can get $\frac{1}{2}G_{2^m \cdot s} = 1 + a \cdot 2^e$, where a is an integer. Then, one has

$$\begin{aligned} \frac{1}{2}G_{2^{m+1} \cdot s} &= \frac{1}{2}(G_{2^m \cdot s}^2 - 2) \\ &= \frac{1}{2}((2 + a \cdot 2^e)^2 - 2) \\ &= a^2 \cdot 2^{2e+1} + a \cdot 2^{e+2} + 1. \end{aligned}$$

As $2e + 1 \geq e + 2$, Eq. (26) can be obtained. \square

Lemma 4. If $G_s = 0 \pmod{2^e}$ and

$$\begin{cases} H_{2^m \cdot s} = 0 \pmod{2^e}, \\ H_{2^m \cdot s} \neq 0 \pmod{2^{e+1}}, \end{cases} \quad (27)$$

$$(28)$$

one has

$$H_{2^{m+1} \cdot s} = 0 \pmod{2^{e+1}}. \quad (29)$$

Proof. From Lemma 1 and

$$H_{2^{m+1} \cdot s} = H_{2^m \cdot s} \cdot G_{2^m \cdot s},$$

one can get Eq. (29). \square

Lemma 5. Equation

$$\mathbf{C}^{T_e} \cdot \begin{bmatrix} x_0 \\ y_0 \end{bmatrix} \pmod{2^e} = \begin{bmatrix} x_0 \\ y_0 \end{bmatrix}$$

holds if and only if

$$\mathbf{C}^{T_e} \cdot \begin{bmatrix} 2x_0 \\ 2y_0 \end{bmatrix} \pmod{2^{e+1}} = \begin{bmatrix} 2x_0 \\ 2y_0 \end{bmatrix},$$

Proof. This proof is straightforward from the elementary properties of congruences summarized in [20, P.61]. \square

Proposition 1. There exist a threshold value of e , e_s , satisfying

$$N_{T_c, e} = N_{T_c, e_s} \quad (30)$$

when $e \geq e_s$, where $N_{T_c, e}$ is the number of cycles of period T_c of Cat map over $(\mathbb{Z}_{2^e}, +, \cdot)$.

Conjecture 1. There exist a threshold value of e , e_s , and that of the length of cycles in F_e , T_s , making the number of cycles with length T_c in F_e and that with length $2T_c$ in F_{e+1} satisfy

$$2N_{T_c, e} = \begin{cases} N_{2T_c, e+1}, & \text{if } T_c \geq T_s; \\ 2N_{T_c, e_s}, & \text{if } T_c < T_s, \end{cases} \quad (31)$$

when $e \geq e_s$.

The infinite number of unstable periodic orbits (UPO's) of a chaotic system constitute its skeleton [21]. In a finite-precision domain, any periodic orbit is a cycle (See Property 3). Its stability is dependent on change trend of its distance with the

neighboring states in the phase space. To show the relative positions among different cycles, we depicted real image of the SMN shown in Fig. 1c) in Fig. 6. Note that some states may be located in different cycles due to the finite-precision effect. The main result obtained in [16], i.e. Eq. (5), describes the number of different possible Cat maps owning a specific period, which has no any relationship with the number of cycles and distance between a cycle and its neighboring states. So, it cannot help to identify unstable periodic orbits of the original chaotic cat map at all.

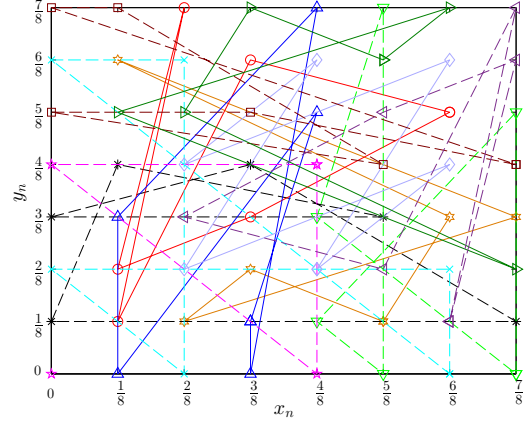


Fig. 6: Portrait of GDCM (2) with $N = 2^3$ where $(p, q) = (1, 3)$.

III. CONCLUSION

This paper analyzed the structure of the 2-D generalized discrete Cat map by establishing its functional graph. The impacting points claimed in the paper can be contradicted by the following conclusions: There exists non-negligible number of short cycles no matter what the period of the whole Cat map is. Knowledge of period distribution of the whole Cat map can not provide any help for detection and identification of its UPO. Although the precise cycle distribution of the generalized discrete Cat map has also been disclosed perfectly.

REFERENCES

- [1] L. Chen and S. Wang, "Differential cryptanalysis of a medical image cryptosystem with multiple rounds," *Computers in Biology and Medicine*, vol. 65, pp. 69–75, Oct 2015.
- [2] M. Farajallah, S. E. Assad, and O. Deforges, "Fast and secure chaos-based cryptosystem for images," *International Journal of Bifurcation and Chaos*, vol. 26, no. 2, p. Article number 1650021, FEB 2016.
- [3] A. Kanso and M. Ghebleh, "A structure-based chaotic hashing scheme," *Nonlinear Dynamics*, vol. 81, no. 1-2, pp. 27–40, Jul 2015.
- [4] M. Falcioni, L. Palatella, S. Pigolotti, and A. Vulpiani, "Properties making a chaotic system a good pseudo random number generator," *Physical Review E*, vol. 72, no. 1, 2, p. Article number 016220, JUL 2005.
- [5] L. Barash and L. Shchur, "Periodic orbits of the ensemble of Sinai-Arnold cat maps and pseudorandom number generation," *Physical Review E*, vol. 73, no. 3, 2, p. art. no. 036701, MAR 2006.
- [6] T. Yarmola, "An example of a pathological random perturbation of the cat map," *Ergodic Theory and Dynamical Systems*, vol. 31, no. 6, pp. 1865–1887, Dec 2011.
- [7] D.-I. Curiac and C. Volosencu, "Path planning algorithm based on Arnold cat map for surveillance UAVs," *Defence Science Journal*, vol. 65, no. 6, pp. 483–488, Nov 2015.

- [8] V. I. Arnol'd and A. Avez, *Mathematical methods of classical mechanics*. New York: W. A. Benjamin, 1968.
- [9] G. Chen, Y. Mao, and C. K. Chui, "A symmetric image encryption scheme based on 3D chaotic cat maps," *Chaos Solitons & Fractals*, vol. 21, no. 3, pp. 749–761, Jul 2004.
- [10] H. Kwok and W. K. Tang, "A fast image encryption system based on chaotic maps with finite precision representation," *Chaos, Solitons & Fractals*, vol. 32, no. 4, pp. 1518–1529, 2007.
- [11] Y. Wu, Z. Hua, and Y. Zhou, " N -dimensional discrete cat map generation using laplace expansions," *IEEE Transactions on Cybernetics*, vol. 46, no. 11, pp. 2622–2633, Nov 2016.
- [12] F. J. Dyson and H. Falk, "Period of a discrete cat mapping," *The American Mathematical Monthly*, vol. 99, no. 7, pp. 603–614, 1992.
- [13] J. Bao and Q. Yang, "Period of the discrete arnold cat map and general cat map," *Nonlinear Dynamics*, vol. 70, no. 2, pp. 1365–1375, Oct 2012.
- [14] F. Chen, K.-W. Wong, X. Liao, and T. Xiang, "Period distribution of generalized discrete arnold cat map for $N = p^e$," *IEEE Transactions on Information Theory*, vol. 58, no. 1, pp. 445–452, Jan 2012.
- [15] F. Chen, X. Liao, K.-W. Wong, Q. Han, and Y. Li, "Period distribution analysis of some linear maps," *Communications in Nonlinear Science and Numerical Simulation*, vol. 17, no. 10, pp. 3848–3856, Oct 2012.
- [16] F. Chen, K.-W. Wong, X. Liao, and T. Xiang, "Period distribution of the generalized discrete arnold cat map for $N = 2^e$," *IEEE Transactions on Information Theory*, vol. 59, no. 5, pp. 3249–3255, May 2013.
- [17] —, "Period distribution of generalized discrete arnold cat map," *Theoretical Computer Science*, vol. 552, pp. 13–25, Oct 2014.
- [18] M. Hall, *The Theory of Groups*. The Macmillan Co., New York, 1959.
- [19] R. Bohme and C. Keiler, "On the security of "a steganographic scheme for secure communications based on the chaos and the euler theorem"," *IEEE Transactions on Multimedia*, vol. 9, no. 6, pp. 1325–1329, 2007.
- [20] G. H. Hardy and E. M. Wright, *An introduction to the theory of numbers*, 6th ed. Oxford OX2 6DP, UK: Oxford University Press, 2008.
- [21] R. L. Davidchack and Y.-C. Lai, "Efficient algorithm for detecting unstable periodic orbits in chaotic systems," *Physical Review E*, vol. 60, no. 5, pp. 6172–6175, 1999.